AIP | Applied Physics Letters

Characterization of spin valves fabricated on opaque substrates by optical ferromagnetic resonance

A. Barman, V. V. Kruglyak, R. J. Hicken, C. H. Marrows, M. Ali et al.

Citation: Appl. Phys. Lett. **81**, 1468 (2002); doi: 10.1063/1.1501159
View online: http://dx.doi.org/10.1063/1.1501159
View Table of Contents: http://apl.aip.org/resource/1/APPLAB/v81/i8
Published by the American Institute of Physics.

Related Articles

Direct method for measuring the canting angle of magnetization
J. Appl. Phys. 113, 023902 (2013)

Direct measurements of field-induced strain at magnetoelectric interfaces by grazing incidence x-ray diffraction
Appl. Phys. Lett. 102, 011601 (2013)

Spin-polarization reversal at the interface between benzene and Fe(100)
J. Appl. Phys. 113, 013905 (2013)

Investigation of induced Pt magnetic polarization in Pt/Y3Fe5O12 bilayers
Appl. Phys. Lett. 101, 262407 (2012)

Spin precession modulation in a magnetic bilayer
Appl. Phys. Lett. 101, 262406 (2012)

Additional information on Appl. Phys. Lett.

Journal Homepage: http://apl.aip.org/
Journal Information: http://apl.aip.org/about/about_the_journal
Top downloads: http://apl.aip.org/features/most_downloaded
Information for Authors: http://apl.aip.org/authors

ADVERTISEMENT

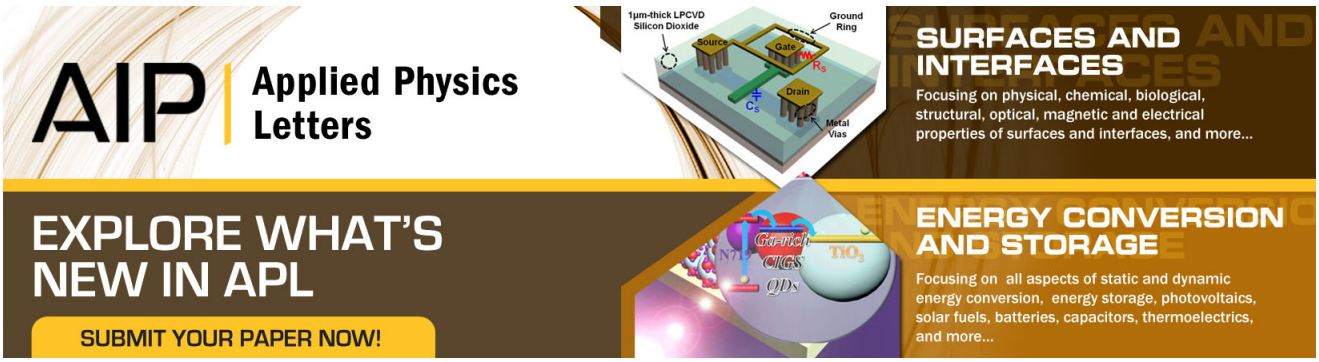

Characterization of spin valves fabricated on opaque substrates by optical ferromagnetic resonance

A. Barman, V. V. Kruglyak, and R. J. Hicken[a)]
School of Physics, University of Exeter, Stocker Road, Exeter, EX4 4QL United Kingdom

C. H. Marrows, M. Ali, A. T. Hindmarch, and B. J. Hickey
Department of Physics and Astronomy, University of Leeds, Leeds, LS2 9JT United Kingdom

(Received 26 March 2002; accepted for publication 25 June 2002)

We have used a transmission line deposited on a transparent substrate to deliver an optically triggered magnetic field pulse to a spin valve structure deposited upon an opaque substrate. The ensuing ferromagnetic resonance oscillations have been studied in optical pump-probe experiments in which the probe passes through the transmission line substrate. The resonance frequencies have been modeled by solving the Landau–Lifshitz equation and are used in determining the anisotropy, exchange bias, and interlayer coupling parameters of the sample. © *2002 American Institute of Physics.* [DOI: 10.1063/1.1501159]

As bit rates in magnetic disk drives and magnetic random access memory (MRAM) circuits increase, ultrafast magnetization dynamics is becoming increasingly important.[1,2] Optical pump-probe spectroscopy is a powerful technique for studying picosecond dynamics in the time domain.[3–5] The sample is pumped by an optically triggered magnetic field pulse and probed by a linear or nonlinear magneto-optical Kerr effect (MOKE) measurement. The focused probe is suited to small inhomogeneous samples, and optical ferromagnetic resonance (FMR) measurements have been demonstrated on single layer thin films and patterned structures.[1,3–5] Samples were either deposited on to the transmission line structure, or on transparent substrates placed face down on the transmission line with the sample being probed through the sample substrate.[1,3,5] We report on how a transmission line fabricated on a glass substrate may be placed on top of any sample, and the sample response probed through the glass.

We have studied a series of spin valve grown on silicon substrates. The spin valve consists of two ferromagnetic (FM) layers separated by a nonmagnetic spacer layer. One FM layer is pinned in a saturated magnetic state by the exchange bias field from an antiferromagnetic layer. The device used to generate the pulsed magnetic field was fabricated by a photolithographic lift-off technique and is shown in Fig. 1. It consists of a switch (Au on intrinsic GaAs) connected by foil straps to a transmission line (Al on glass). The switch is an interdigitated structure with fingers of 10 μm width and separation, and the transmission line tracks have 30 μm width and separation at the sample position. A bias voltage of 20 V is applied to one end of the transmission line while the switch is connected to the other end. Two 47 Ω surface mount resistors terminate the transmission line so as to absorb the current pulse. The transmission line is placed face down and clamped lightly to the sample. Between the tracks the current pulse generates an out of plane pulsed magnetic field. The spin valves were grown by magnetron sputtering within a magnetic field of approximately 200 Oe. The nominal sample structure was Si (100)/Ta (50 Å)/$Ni_{81}Fe_{19}$ (50 Å)/Cu (dÅ)/Co (50 Å)/IrMn (100 Å)/Ta (30 Å) where $d=10$, 20, and 30 Å for samples S1, S2, and S3, respectively. Optical FMR measurements were performed at a wavelength of 790 nm by means of a pump-probe technique described in detail elsewhere.[5] The pump pulse was used to trigger the switch shown in Fig. 1. The pulsed magnetic field typically has a rise time of 30 ps, a decay time of 2 ns[6] and a peak magnitude of about 13 Oe. The p-polarized probe beam is focused through the glass substrate to a 15 μm diameter spot on the sample surface between the tracks of the transmission line. The pump beam is chopped, and the Kerr rotation of the probe beam is measured in an optical bridge using a lock-in amplifier.

Typical scans acquired from samples S1 and S3 are shown in Fig. 2(a). A static magnetic field of up to 1 kOe was applied to the sample. The FMR mode frequencies are determined from fast Fourier transforms (FFT) of the time domain data. The FFT power spectra for the data in Fig. 2(a) are shown in Fig 2(b). It is clear that there are two modes for S3 at 3.2 and 4.45 GHz, while for S1 there is one mode at

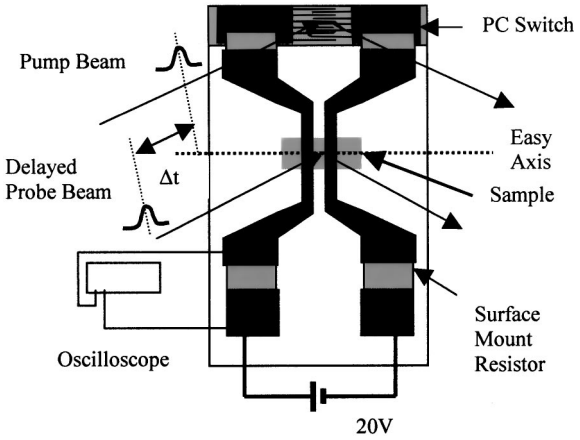

FIG. 1. A schematic of the transmission line structure is shown. The plane of incidence is in the horizontal direction.

[a)]Electronic mail: r.j.hicken@exeter.ac.uk

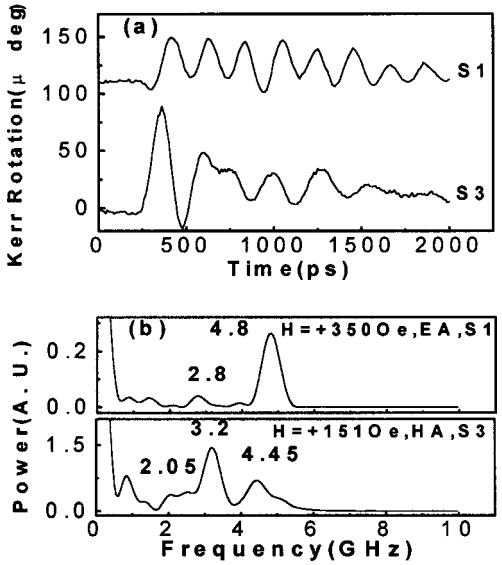

FIG. 2. (a) Typical time resolved spectra for S1 and S3 are shown. (b) The corresponding fast Fourier transform power spectra are shown.

4.8 GHz. The peaks at 2.8 GHz for S1 and at 2.05 GHz for S3 are associated with reflections of the current pulse at the various junctions of the transmission line. These peaks may be easily identified and rejected since their position does not depend upon the static magnetic field. Where necessary the power spectra have been fitted with a multiple peak profile to isolate the frequency of the FMR modes. The error bars in later figures take account of the uncertainty introduced by this procedure.

Static MOKE loops were acquired at 633 nm with the magnetic field applied both parallel and perpendicular to the direction in which the magnetic field was applied during the sample growth. These are expected to be the easy axis (EA) and hard axis (HA) directions, respectively. The loops are shown in the insets of Figs. 3 and 4. While for S2 (not shown) and S3, separate switching of the Cobalt and $Ni_{81}Fe_{19}$ (permalloy) layers was clearly observed in the EA loops, for S1 only a single switching field was observed. For all three samples we observed a clear shift of the center of the loops from zero field. For S2 and S3 only the EA loop was shifted, while for S1 the HA loop was also slightly shifted. This suggests that the exchange bias field is parallel to the direction of the growth field for S2 and S3 but canted at a small angle to the growth field in S1.

FMR measurements were performed with the static field applied parallel to the EA and HA. In Figs. 3 and 4 the dependence of the mode frequencies upon the static field (H) is shown for S1 and S3. For S1, only a single mode was observed while for S2 (not shown) and S3 there were two modes. The cusps and turning points are correlated with features in the hysteresis loops. In order to model the field dependence of the frequencies we have solved the Landau-Lifshitz (LL) equation for a coupled trilayer system[7]

$$\frac{\partial \mathbf{M}_i}{\partial t} = -|\gamma_i|[\mathbf{M}_i \times \mathbf{H}_{\text{eff}\,i}], \tag{1}$$

where $i=1, 2$ correspond to the cobalt and permalloy layers

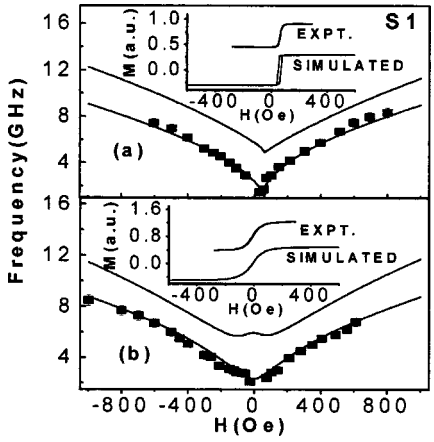

FIG. 3. Experimental (points) and simulated (curves) FMR frequencies for S1 with (a) H along the EA and (b) H along the HA of the sample. The inset shows the corresponding experimental and simulated hysteresis loops.

respectively and γ_i and $\mathbf{M}_i$ are the gyromagnetic ratio and magnetization in layer i, respectively. The total effective magnetic field $\mathbf{H}_{\text{eff}\,i}$ can be written as

$$\mathbf{H}_{\text{eff}\,i} = -\frac{1}{M_i}\nabla_{ui} E_{\text{eff}\,i}, \tag{2}$$

where $E_{\text{eff}\,i}$ is the effective energy per unit volume of layer i. The total magnetic free energy per unit area can be written as

$$E = \sum_{i=1,2} d_i[-\mathbf{M}_i\cdot\mathbf{H} - K_i(\mathbf{u}_i\cdot\mathbf{k}_i)^2 - M_i(\mathbf{u}_i\cdot\mathbf{b}_i)H_{ei} + 2\pi M_i^2 u_{iz}^2] + A_{12}\mathbf{u}_1\cdot\mathbf{u}_2, \tag{3}$$

where d_i, K_i, and H_{ei} are the thickness, uniaxial anisotropy constant, and exchange bias field of each layer. The unit vectors $\mathbf{u}_i$, $\mathbf{k}_i$, and $\mathbf{b}_i$ are parallel to the magnetization, uniaxial anisotropy axis, and exchange bias field, respectively, in each layer, while A_{12} is the interlayer coupling constant. The static solution is first obtained by minimizing Eq. (3) using a steepest descents method. We then solve the LL equation within the small angle approximation to obtain the mode frequencies

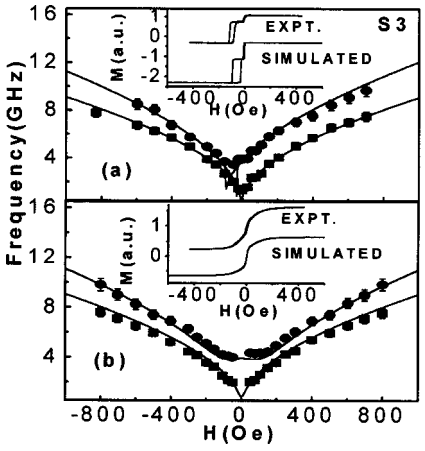

FIG. 4. Experimental (points) and simulated (curves) FMR frequencies are shown for S3 with (a) H along the EA and (b) H along the HA of the sample. The inset shows the corresponding experimental and simulated hysteresis loops.

TABLE I. Parameters obtained from simulating the hysteresis loop and FMR data. Subscripts 1 and 2 refer to the Co and permalloy layers, respectively.

	$2K_1/M_1$ (Oe)	$2K_2/M_2$ (Oe)	$4\pi M_1$ (kOe)	$4\pi M_2$ (kOe)	H_{e1} (Oe)	φ_{e1} (deg)	A_{12} (erg/cm^2)
S1	72.7	3.38	13.8	8.17	95	165	−0.05
S2	52.2	3.08	14.4	9.80	95	180	−0.0015
S3	54.5	2.4	13.8	9.42	75	180	−0.003

$$(\omega)^2_{\pm}=\tfrac{1}{2}[(J)\pm\sqrt{(J)^2+4(G_1G_2-B_1B_2)(C_1C_2-F_1F_2)}], \tag{4}$$

where $J=F_1G_1+F_2G_2+B_1C_2+B_2C_1$,

$$F_i=\gamma_i\left[H\cos\phi_i+H_{ei}\cos(\phi_i-\phi_{ei})+\frac{2K_i}{M_i}\times\cos 2(\phi_i-\phi_{ki})-\frac{A_{12}}{M_id_i}\cos(\phi_1-\phi_2)\right]$$

$$G_i=\gamma_i\left[H\cos\phi_i+H_{ei}\cos(\phi_i-\phi_{ei})+\frac{2K_i}{M_i}\times\cos^2(\phi_i-\phi_{ki})+4\pi M_i-\frac{A_{12}}{M_id_i}\cos(\phi_1-\phi_2)\right]; \tag{5}$$

$$B_i=\frac{\gamma_iA_{12}}{M_id_i};\quad C_i=B_i\cos(\phi_1-\phi_2)$$

and ϕ_i, ϕ_{ei}, and ϕ_{ki} are the angles that the static magnetization, the exchange bias field, and the uniaxial anisotropy make with the external field. In the absence of interlayer coupling, the mode frequencies correspond to uniform precession modes of the Co and permalloy layers. Otherwise the two modes correspond to collective excitations of the trilayer in which the layer magnetizations precess either in or out of phase. The magneto-optical response from the two layers may cancel for the out of phase mode, particularly in the presence of strong ferromagnetic coupling[8] as in S1. The loops obtained from the static solution are shown in the inset of Figs. 3 and 4 along with the measured loops. The loops are used to provide an initial determination of the anisotropy, exchange bias, and interlayer coupling fields. The simulated frequencies are shown as solid lines in Figs. 3 and 4. The measured and calculated frequencies are in good agreement. Table I shows the parameter values obtained by simulating the loops and FMR frequencies. The EA directions lie parallel to the direction of the growth field. Values of 2.1 and 2.0 were obtained for the g factors of Co and permalloy, respectively. The Co anisotropy constant was somewhat larger in S1 compared to S2 and S3. The demagnetizing fields, $4\pi M_i$, are smaller than the bulk values (17.9 kOe for Co and about 10 kOe for permalloy) in all three samples. For S2 and S3 the measured and simulated frequencies still agree within experimental error as the values of $4\pi M_i$ are adjusted by about $\pm 5\%$. Due to the absence of a stepped loop, and a second mode in the FMR data, acceptable agreement with the FMR data from S1 was obtained with values of $4\pi M_2$ in the range 8.0–9.6 kOe, although the value in Table I gave the best agreement. The reduced demagnetizing fields may be due to either reduced magnetization or thickness dependent anisotropy that favors perpendicular magnetization. The small value of $4\pi M_2$ in S1 is most likely associated with a somewhat smaller thickness for the permalloy layer in this sample. Two interesting features are the canting of the exchange bias field by 15° from the growth field, and the strong ferromagnetic interlayer coupling in S1. Canting of the exchange bias field has been observed in spin valve structures before[9] and strong ferromagnetic coupling is to be expected through such thin Cu layers perhaps due to pinhole coupling.

In conclusion, we have demonstrated that a transmission line fabricated on a transparent substrate allows optical pump-probe experiments to be made on samples grown on any opaque substrate. We have shown that the measured FMR frequencies can be used to determine the magnetic parameters of a multilayered magnetic structure such as a spin valve. We anticipate that the technique may now be applied to a wide variety of microstructured multilayered samples.

The authors gratefully acknowledge the assistance of Dr. M. Rahman and A. Kundrotaite in the fabrication of photoconductive switches, of Dr. S. E. Huq for the fabrication of a photomask, and of the EPSRC in the provision of financial support.

[1] B. C. Choi, G. E. Ballentine, M. Belov, and M. R. Freeman, Phys. Rev. B **64**, 144418 (2001).
[2] R. H. Koch, J. G. Deak, D. W. Abraham, P. L. Trouilloud, R. A. Altman, Y. Lu, W. J. Gallagher, R. E. Scheuerlein, K. P. Roche, and S. S. P. Parkin, Phys. Rev. Lett. **81**, 4512 (1998).
[3] W. K. Hiebert, A. Stankiewicz, and M. R. Freeman, Phys. Rev. Lett. **79**, 1134 (1997).
[4] T. M. Crawford, P. Kabos, and T. J. Silva, Appl. Phys. Lett. **76**, 2113 (2000).
[5] J. Wu, D. S. Schmool, N. D. Hughes, J. R. Moore, and R. J. Hicken, J. Appl. Phys. **91**, 278 (2002).
[6] R. J. Hicken and J. Wu, J. Appl. Phys. **85**, 4580 (1999).
[7] P. E. Wigen, Z. Zhang, L. Zhou, M. Ye, and J. A. Cowen, J. Appl. Phys. **73**, 6338 (1993).
[8] R. J. Hicken, A. J. R. Ives, D. E. P. Eley, C. Daboo, J. A. C. Bland, J. R. Childress, and A. Schuhl, Phys. Rev. B **50**, 6143 (1994).
[9] C. H. Marrows, F. E. Stanley, and B. J. Hickey, J. Appl. Phys. **87**, 5058 (2000).